Sixth International Symposium on Marine Propulsors
smp'19, Rome, Italy, May 2019

Measurements of the hydro-elastic behaviour of flexible composite propellers in non-uniform flow at model and full scale

Nicola Grasso[1], Rink Hallmann[1], Thomas Scholcz[1], Gert-Jan Zondervan[1], Pieter Maljaars[2], Rogier Schouten[1]

[1]Maritime Research Institute Netherlands (MARIN), Wageningen, The Netherlands
[2]Department of Maritime & Transport Technology, Delft University of Technology (TUDelft), Delft, The Netherlands

ABSTRACT

In this paper, new developments in the measurement technology of the hydro-elastic response of flexible composite propellers are described. The first part of this paper covers the testing of two composite propellers operating in non-uniform flow in a cavitation tunnel. The flow field was created by a wake generator mounted inside the tunnel and designed by means of computational fluid dynamics (CFD). The obtained wake field was then validated through Particle Image Velocimetry (PIV) flow measurements. The actual composite propeller tests were carried out with Digital Image Correlation (DIC) technique to measure the deflection of the flexible blades during the full propeller revolution. This paper describes both the test setup and the challenges encountered in the data processing.

Besides the laboratory tests, this paper covers the full scale test measurement campaign performed for a flexible, composite propeller installed on one of the Royal Netherlands Navy's diving support vessels within the Greenprop project. The deformation of the propeller blades was measured optically with DIC and two underwater cameras installed on the vessel's rudder providing stereoscopic images of the propeller blades. Despite challenges such as the high rotational speed of the propeller, underwater visibility, cavitation, scarcity of natural light and vibrations, excellent measurement quality was achieved as the propeller blade deformations were delivered with an accuracy comparable to the tests in the laboratory. In addition, observations of the propeller cavitation pattern were collected with an outstanding image quality.

Keywords

Composite propeller, Hydro-elasticity, Digital Image Correlation, Particle Image Velocimetry, Computational Fluid Dynamics, Full scale measurements

1 INTRODUCTION

The application of fibre-reinforced composite materials could potentially lead to important performance enhancements of marine propellers. The exploitation of the bend-twist coupling effects of composites has been proposed as a property that can simultaneously improve efficiency as well as reducing cavitation nuisance, which is impossible to obtain for metallic propellers. For optimum propellers, reducing cavitation nuisance always goes at the expense of efficiency, and vice versa.

There is a crucial lack of feedback from sea trials on the full scale behaviour of composite propellers in the operational environment. Knowledge on the operational hydro-elastic behaviour of flexible propellers is required to exploit the full potential of this technology. The development and validation of accurate computational tools together with designing and testing of flexible propellers in laboratory and full scale conditions are key steps to obtain this knowledge.

Significant progress has been made in the experimental investigation of the behaviour of flexible composite propellers in realistic environmental conditions. A decade ago, MARIN developed and applied Digital Image Correlation (DIC) for the measurement of the deformation of flexible propeller blades for model propellers in the uniform flow of a cavitation tunnel. Recently, this test method was applied to validate hydro-structural simulation tools for the analysis and design of composite propellers. Work in the Greenprop project on the validation of a BEM-FEM coupled simulation code using the results of these measurements is reported by Maljaars et al. (2017) presented at the previous SMP'17 symposium. Results of a first pilot study using the DIC technique for a deforming propeller in the unsteady flow behind a ship model, together with an outline of new design opportunities for composite propellers was presented at the same occasion, see Zondervan et al. (2017).

Ship propellers are operating in highly unsteady wake fields of ships with flow oscillations at widely varying scales. Vortices that are shed from appendages like stabilizer fins, shaft brackets, shaft bossing wander through the propeller plane as a result of ship motions and sea waves. At smaller scales the turbulence generated by the boundary layers of the hull or the boundary layer of the propeller itself is causing highly unsteady loading of the propellers as well. For traditional metallic propellers the influence of these loads is well covered by the safety

factors in the strength rules developed by the classification societies. How flexible composite propellers behave in these 'normal' wake fields is still the big question, therefore the hydro-elastic behaviour of flexible propellers must be assessed also in the presence of such unsteadiness and the feedback from full scale measurements is extremely important.

The objective of this paper is to provide an overview of recent experimental techniques on the measurement of blade deformations of composite propellers. We present the methods applied in two test campaigns involving the measurement of the deformations of flexible composite propellers in unsteady inflow conditions. The first one considers the designed unsteady flow by a wake generator in a cavitation tunnel. The second considers measurements applied in an actual full scale trial campaign where for the first time the deformations of a full scale composite propeller are measured.

2 CAVITATION TUNNEL TESTS

2.1 Overview

A test set-up was developed to generate high quality measurement of unsteady blade deformation for a series of flexible composite propellers in the confinement of a cavitation tunnel. The goal of the experiments was to use the measured data as validation for unsteady BEM-FEM simulations of the hydro-elastic behaviour of the propeller blades. This set-up consisted of two high speed camera's that covered a large part of the propeller revolution. Two flexible model propellers were tested operating in the unsteady wake field of a wake generator. The desired properties of the generated wake field was a single, reasonably wide axial wake peak, which would lead to a significant deformation of the propellers. This wake field was designed using CFD as described in the next section.

Three geometrically identical 2-bladed propellers with a diameter of 0.34 meters were used in this test campaign. One of the propellers was made of isotropic bronze material, while the other two presented two different composite laminate lay-up, as follows:

- Bronze propeller: Isotropic NIAB material
- Propeller 45: [+45°/-45°] laminate lay-up.
- Propeller 90: [0°/90°] laminate lay-up.

The 0°direction of the laminate lay-up is parallel to the z-axis of the propeller blade coordinate system, as indicated in Figure 1.

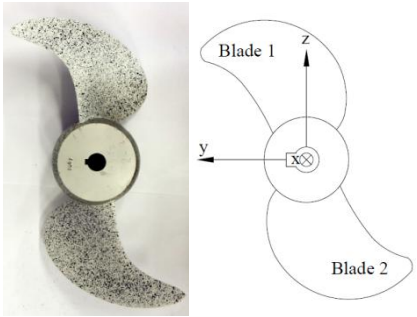

Figure 1: Photo of one of the tested propellers and definition of the coordinate system

2.2 Design of a wake field generator

A wake generator is used to obtain a propeller wake-field with the desired properties. A sketch of the model setup is shown in Figure 2. It must be noted that, contrarily to what is indicated in Figure 2, the wake generator was finally mounted on the floor of the cavitation tunnel.

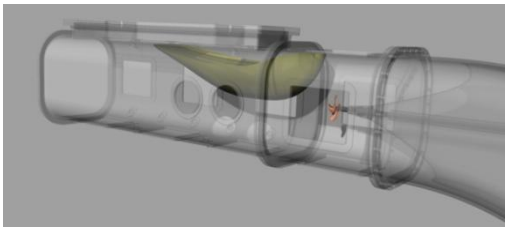

Figure 2:Wakefield generator (yellow) and propeller (bronze) in the MARIN water tunnel. The water is flowing from left to right.

The design of the wake-field generator was carried out using a simple optimisation procedure, whose steps are:

1. Definition of the optimisation requirements and shape parameterisation,
2. Application of an optimisation method
3. Review the optimised design.

The target wake-field was developed to enhance the hydro-elastic response of the propeller, therefore it was not designed to be representative of a typical ship-shaped hull. The requirements for the wake-field are the following:

a) The wake-peak should be relatively deep with an axial speed u_{min}/u_{ref} of approximately 0.4 – 0.6.
b) High harmonics should be avoided.

To comply with these requirements, the target wake-field is composed of three harmonics which amplify each other at the location of the wake-peak and dampen each other outside this region. The target wake-field is shown in Figure 3.

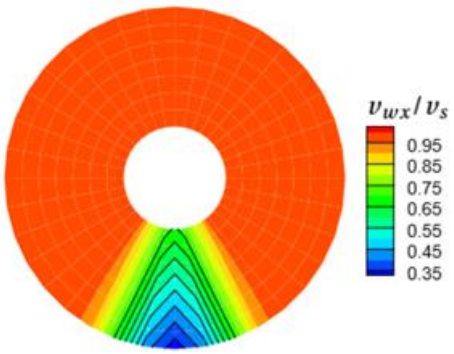

Figure 3: Target nominal wake-field at 6.75 m/s (only axial)

The optimization procedure starts with an initial generator geometry which is drawn in red in Figure 4. A deformer box was defined around this geometry which allows to scale the geometry length, width and height of the surface. A fourth parameter controls the axial distance of the entire wake field generator with respect to the propeller. The 4D design space is denoted by D_x. Some of

the possible shape variations are shown in black in Figure 4.

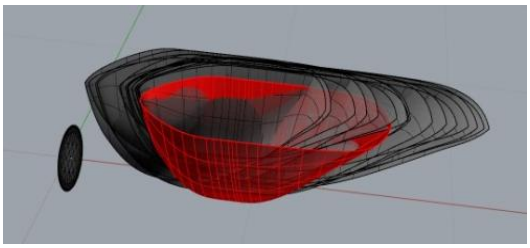

Figure 4: Selection of shape variations in the design space. The water is flowing from right to left. The initial generator geometry is shown in red.

2.2.1 Optimisation method

The incompressible viscous CFD solver ReFRESCO[1] was used to compute the wake that results from the wake field generator. A steady flow was simulated at a constant speed of 6.75 m/s. The water velocity for the optimisation study was chosen to be at the operational limit of the cavitation tunnel. At this velocity a maximum deformation of the flexible propeller can be expected, while minimising the chance of occurring of a cavitating leading edge vortex.

To design the wake field generator we define:

$$\Delta_{wake}(\boldsymbol{x}) = wake_{target} - wake_{CFD}(\boldsymbol{x}),$$

Where $\Delta_{wake}(x)$ is the difference between the target wake field ($wake_{target}$) and the computed wake field ($wake_{CFD}(x)$) for $x \in D_x$. Minimising $\Delta_{wake}(x)$ in the L_2-norm results in the single objective optimisation problem:

$$\min_{\boldsymbol{x}} \|\Delta_{wake}(\boldsymbol{x})\|, \ \boldsymbol{x} \in D_x,$$

This optimisation problem can be solved by an optimisation algorithm. In this case the Single Objective Genetic Algorithm (SOGA) algorithm available in Sandia's National Laboratories optimisation toolkit DAKOTA was used. More information on this algorithm can be found in the work of Adams et al. (2017).

2.2.2 Design review

The convergence of the SOGA never reaches the target but the best approximation was found in about 12 SOGA generations. The resultant optimised wake-field can be observed in Figure 5. This is the best candidate in the design space and satisfies the optimisation requirements as u_{min} is approximately 0.5 and the presence of higher harmonics is limited.

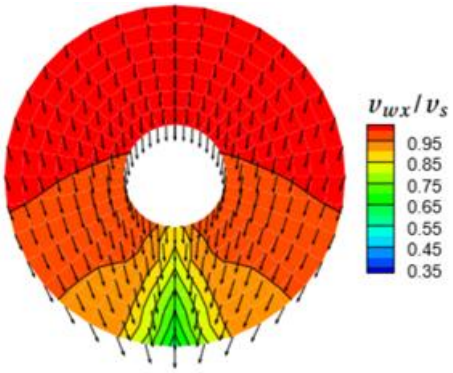

Figure 5: ReFRESCO solution of the nominal wake-field at 6.75 m/s that results from the optimised wake-field generator.

2.3 Wake measurements

Particle Image Velocimetry (PIV) is the selected measurement technique to determine realised nominal wake field in the cavitation tunnel. This measurement technique uses image data of a thin plane illuminated by a laser as a base for the measurement. The recorded images are processed to obtain the velocity fields. In this process, the background light was removed and the displacement observed with the two camera's was determined for each camera and then combined to obtain the velocity fields. Polyamide particles of 30µm size were introduced in the water to ensure than enough seeding is present to carry out the measurements.

A dedicated PIV setup was constructed in the cavitation tunnel for this test campaign. The cameras were positioned upstream of the propeller plane and a laser sheet was shone through that plane from a custom made window positioned at the bottom of the tunnel (see Figure 6 and Figure 7).

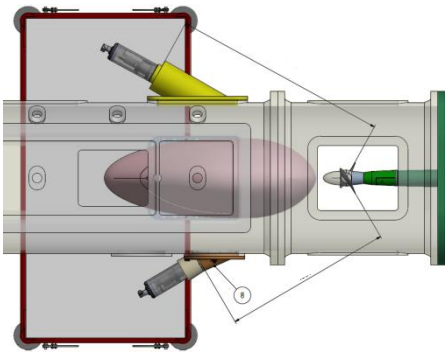

Figure 6: PIV measurement setup in the cavitation tunnel

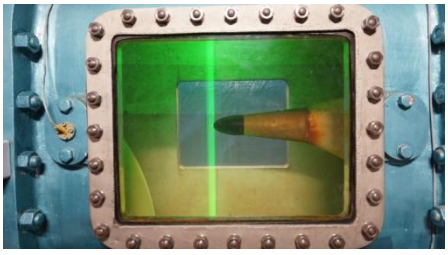

Figure 7: Laser sheet through the propeller plane

[1] ReFRESCO (www.refresco.org) is a community based open-usage CFD code for the Maritime World. It solves multiphase (unsteady) incompressible viscous flows using Navier-Stokes equations, complemented with turbulence models, cavitation models, and volume-fraction transport equations for different phases(see Vaz et al. 2009).

The measurements were performed at water velocities of 4, 5, 6 and 6.75 m/s and with various time intervals between the consecutive frames. For each of the test conditions, 500 recordings were collected.

In general, similar non-dimensional wake field were observed for all the tested speeds. In Figure 8 the non-dimensional wake field is presented for the test at 6.75 m/s.

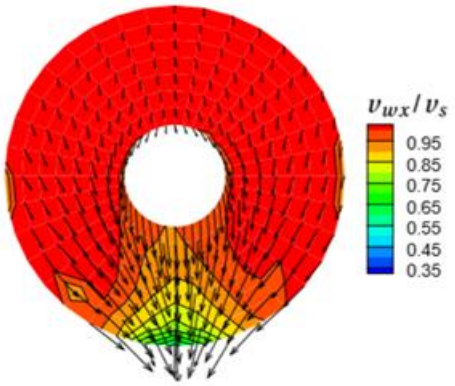

Figure 8: Measured nominal wake field presented at 6.75 m/s.

The comparison between measurements and the predictions provided by CFD shows that the measured wake-peak is considerably stronger and wider than the calculated one with regards to axial velocities. Locally, the measured axial speed is up to 40% lower than calculated. Considerable differences were also found in tangential and radial velocity components about +/- 20% of the water speed.

An assessment of the consequences of such under-prediction of the wake-peak was carried out using MARIN's BEM code PROCAL, see Bosschers et al. (2017). The result is that the lowest tested water velocity had to be slightly increased to avoid the risk of a leading edge vortex on the propeller blades.

2.3.1 Assessment of measurement uncertainty

Quantifying the uncertainty in the resulting velocities is not straightforward. The measurement principle is based on the determination of particle shifts within a certain time interval and such shift can be determined with an accuracy of 0.05 to 0.1 pixel if the recording is of sufficient quality (U95 error estimate, see Westerweel, 2000). This peak detection error has a bias towards an integer number for the displacement, this is called peak locking. If the flow is fluctuating, this error can become partly random and can be reduced if the average of multiple velocity fields is taken. For the purpose of the present work this error is estimated using 0.1 pixel uncertainty in the peak displacement as the upper bound worst case.

Comparison of the two frames for both cameras yields that the average pixel shift is approximately 4.5. The measurement error can be calculated by considering such shift, the geometry of the stereo camera set-up and the method used to combine the two cameras. The resulting uncertainties for the 6.75 m/s with a time interval of 198μs test are computed and presented in Table 1. It can be observed that the expected uncertainty in the axial velocity is ±1.6%. Using a longer time intervals between the frames results in a larger observed shift, but the correlation quality may reduce, while a shorter time interval has a better correlation, but the uncertainty from the determination of the shift is relatively larger.

Table 1: Measurement uncertainties for 6.75 m/s water velocity

Velocity component	u	v	w
Direction	Out-of-plane	Horizontal in-plane	Vertical in-plane
Pixel accuracy [pixel]	±0.1/√2	±0.1/√2	±0.1/√2
Scale [mm/pixel]	0.30	0.17	0.17
Accuracy [mm]	±0.021	±0.012	±0.012
Velocity [m/s]	±0.11	±0.06	±0.06

2.4 Blade deformation measurements

The measurements of the blade deflections are carried out with Digital Image Correlation (DIC). This technique is a full-field image analysis method, based on grey value digital images, that finds the displacements and deformations of an object in three dimensional space (Sutton et al. 2009). During displacement and deformation of an object, the method tracks and correlate the gray value pattern in small square groups of pixels called subsets. If all displacements are taking place in one plane, only one camera can be used to accurately track the subsets. If displacements take place in three-dimensional space, two or more cameras must be used.

Besides the measurements on flexible propellers, at MARIN this technique was applied to a diverse range of problems, such as the measurement of the deformation of a flexible ship model, the strain of the foam structure of an LNG containment system under wave impacts, (see Van de Bunt et al, 2011), but also sea wave measurements and the behaviour of large flexible floaters in waves (for the latter see Sterenborg et al, 2019).

Commercial software Vic3D was used for the DIC analyses described in this paper. This software is capable to perform the camera system calibration, calculate the displacements for a series of images and output the results for further post-processing. When the correlation is performed on the images of the undeformed object, also called reference images, the shape of the propeller blades without loading can be identified. Under loading the subsets will shift, transform and the displacement of the object can be calculated after comparison with the reference shape.

In order to use the DIC technique, the object surface needs to present a random speckle pattern with no preferred orientation (isotropic) and have a high contrast. The size of the features in the pattern should be large enough to distinguish them as distinct features. If not naturally present, such speckles can be sprayed, painted or projected. In Figure 9 examples of speckles sprayed and artificially generated for printing are shown. For more detailed information on DIC, reference is made to Sutton et al (2009).

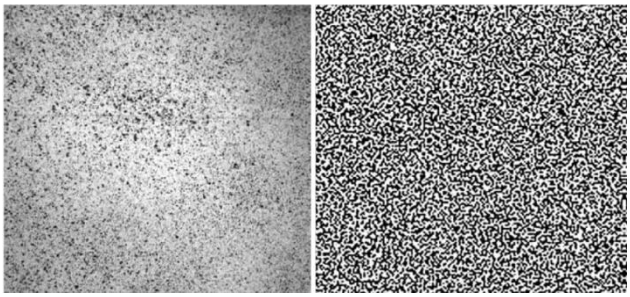

Figure 9: Example of speckle patterns. Left: Speckle pattern created with spray paint. Right: Artificial speckle pattern for printing. (Van de Bunt and Lafeber 2011).

2.4.1 Test setup

The measurement setup installed on the MARIN cavitation tunnel comprises several components summarised in Figure 10. The propeller is mounted on the tunnel shaft, which is connected to an encoder. The encoder sends impulse signals that trigger the strobe lights and the two cameras. The triggering shaft angle was increased with steps of 1 degree over time to gather data during the full propeller revolution.

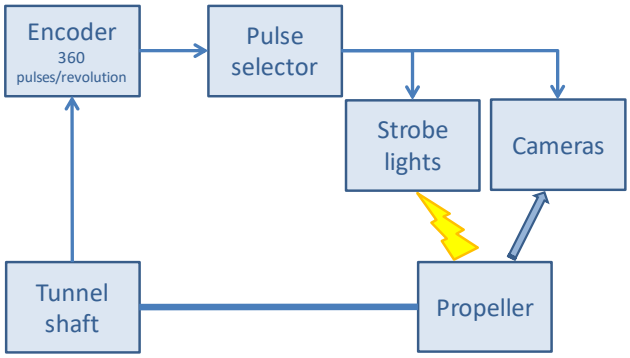

Figure 10: Schematic of the measurement setup

This measurement setup is very similar to the one previously used in the MARIN cavitation tunnel for uniform flow measurements and described by Maljaars et al. (2017). The main difference is that, during those measurements, the two cameras were placed on two separate windows respectively at the side and at the bottom of the tunnel. This positioning guaranteed an optimal view on a single propeller position and a large distance between the cameras, resulting in excellent measurement accuracy. Such setup is not usable for measurements in non-uniform flow as it enables data collection within a very small range of the propeller rotation. This would not provide enough information to properly estimate the influence of the wake field on the blade deflection. With this in mind, the cameras were both placed on a purposely built window at the side of the tunnel window (see Figure 11). This setup provides an optimal view over the full revolution of the propeller; however, as the baseline distance between the cameras is sensibly reduced, a reduction in the measurement accuracy is expected.

Figure 11: Camera setup in the cavitation tunnel

2.4.2 Data post-processing and results

The test matrix included a total of 6 tests with different propeller RPM values and water velocities. For each test, approximately 35 stroboscopic stereo-images were collected every 1 degree of propeller rotation, leading to over 20000 images gathered for each test. One of the challenges was to develop an analysis framework able to effectively manage such a large dataset. Commercial software Vic3D was used for the core DIC analysis, while custom made MATLAB® routines were used to streamline the input and output of the data into the DIC analysis and optimize the workflow for rotating objects.

Another challenge was the handling of the large blade dynamics found during the tests. As the purpose of this test campaign was to provide validation data for a BEM-FEM solver, the objective was to isolate the average periodic deformations and filter out the effects of the non-periodic higher frequency blade vibrations. Such vibrations were mainly generated by the presence of an intermittent cavitating leading edge vortex present in some of the tests, but also hydro-elastic response of the propeller blades and the flow unsteadiness generated by the wake generator and/or the observing window played a role. The handling of such practical challenges paved the way to the development of techniques that are useful in coping with “real world” wake fields, and therefore to the full scale measurements described in the following section of this paper.

A surface averaging procedure was developed to cope with the non-periodic blade dynamics and find the average deflection at each angular position. This method firstly performs a cross-correlation between all the images shot for each angular position to identify and discard “unusual” cases, such as the intermittent cavitation. The remaining images are processed with DIC and the resulting blade surfaces are averaged. This method was

found very effective; however, residual noise in the results is present due to the severity of such dynamics. An example is shown in Figure 12 where four images from the most challenging test are shown. These are shot at 6 o' clock position with the exact same conditions (RPM, tunnel speed and pressure) and large differences in deflection are visible, especially if the cavitating leading edge vortex is present.

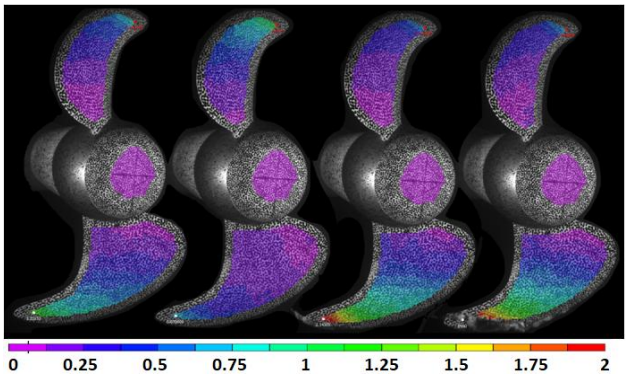

Figure 12: Example of variation in total blade deflection at the tip mainly induced by the cavitating leading edge vortex. All units in mm.

The measurement setup successfully captured the deflection of the propeller blades for almost the full propeller revolution. Only in a few positions the view on the blade was too skewed to produce reliable measurements and therefore were discarded. Some cases with excessive cavitation were also discarded. Signal filtering improved the results considerably for all cases. An example is shown in Figure 13.

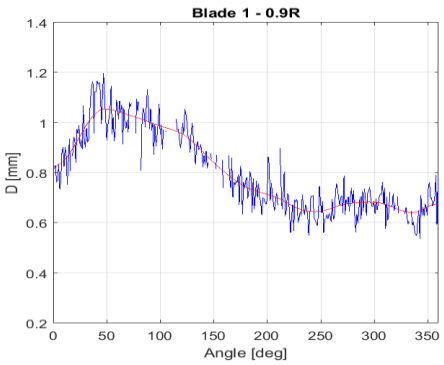

Figure 13: Example of propeller blades deflection at 0.9R.

2.4.3 Assessment of measurement accuracy

To determine the measurement accuracy, a rigid body motion was imposed on the propeller by shifting it along its axis with a spacer ring inserted on the shaft. The average measured shift was 5.2 mm and 5.3 mm for respectively the top and bottom blade, this difference is due to imperfections and tolerances of the spacer ring. Such imperfections complicate the quantification of bias in the measurements. As an educated guess based on the obtained results, DIC projection errors and the user's experience with DIC, such bias is expected to be very small and negligible.

The measurement noise was assessed by correcting the rigid body motion induced with the spacer ring and evaluating the residual deflection. When the view on the surface is skewed, the speckle pattern correlation is more difficult, resulting in an higher noise level, therefore the measurement noise varies with the blade position. Representative cases of "good" and "skewed" views are chosen and the resultant measurement accuracy is reported below as the absolute recorded maximum and the 95% confidence interval assuming the noise as Gaussian distributed.

- "Good" view: $D_{95} = \pm 0.05$ mm
- "Skewed" view: $D_{95} = \pm 0.06$ mm

Such values are considered very good and negligible compared to the noise in the data induced by physical non-periodic blade vibrations, proving the effectiveness of this measurement system.

3 DEFORMATION MEASUREMENTS AT FULL SCALE

3.1 Overview

Understanding the complex hydro-elastic behaviour of composite propellers at full scale is key in the development and validation of numerical tools aimed to propeller design. For this purpose, the Royal Netherlands Navy Diving Support Vessel "Nautilus" (Figure 14) was equipped with a flexible composite propeller and dedicated trials were performed including measurements of the blade deflections for validation of BEM-FEM tools. The details on this validation study can be found in Maljaars et al. (2019). The main particulars of the vessel are:

- Displacement: 217 t
- L: 38.5 m
- B: 8.6 m
- Max speed: 10.5 kn
- Twin screw, with flexible composite propeller installed on portside
- Propeller diameter: 1 meter

The measurements were carried out for two propeller blades at 12 o' clock (wake peak position), 1 o' clock and half past two for several conditions at varying propeller speed and with one and two propellers engaged.

Figure 14: The Diving Support Vessel "Nautilus"

To evaluate the feasibility of the measurement campaign, a pre-study was carried out where the risks related to the practical use of the measurement equipment, the expected cavitation behaviour, the underwater visibility at the trial location and the requirements in terms of illumination and optics were assessed. The study indicated that the project is challenging but feasible and its results were used as input for the engineering of a measurement system based on DIC.

3.2 Design of the measurement system

Two machine vision cameras with high light sensitivity were installed in two separate underwater housings. The camera optics were controlled remotely through a control system comprising 3D printed parts, control engines and gears. Both the hardware and the software of the control system were custom made by MARIN. This allowed to not compromise on the quality of the optics while still retaining the possibility to adjust the lens settings from onboard. The cameras were triggered through a hardware pulse synchronized with the propeller shaft and a software tool to delay the trigger was used to observe the propeller blades at different angles. In addition, ship speed, heading, shaft torque and RPM were also measured.

Natural light was not sufficient to avoid motion blur due to the high tip speed of the propeller, therefore powerful artificial illumination was added. As a first step, underwater lights available on the market were assessed, but unfortunately no items able to provide sufficient light intensity while being reasonably compact were found. The solution was found by developing small custom made subsea strobe lights triggered by an hardware pulse synchronized with the propeller shaft and the camera's. Two sets of 8x lights were prepared at MARIN and mounted respectively on the rudder and on the hull approximately 1 meter portside of the rudder stock. The position of the lights was aimed to an uniform illumination of the propeller hub and the blades at the wake peak position. Excellent results were obtained as no motion blur was visible and an almost uniform illumination of the propeller blade was achieved at the wake peak position.

The design of the cables supports presented challenges in the connection between rudder and hull. Here a slack support was introduced to allow the normal operation of the rudder while minimizing cable fatigue and vortex induced vibrations with small helical strakes.

A clear view on the propeller surface is key in the successful application of DIC. To achieve this while not disturbing the incoming flow, it was necessary to mount the housings on the portside rudder in between the tip and hub cavitating vortices. This led to additional challenges due to limited baseline distance between the cameras and the strong flow causing heavy loads and possible cavitation on the housings. These challenges were tackled through careful positioning of all the items based on the cavitation observations carried out during the feasibility study and a sturdy design of the housing supports, which were also designed to allow the adjustment of both the horizontal and vertical orientation of the cameras. Furthermore, both the adjustment and the removal of the complete measurements system could be carried out by a diver therefore without requiring additional dry-docking. The final cameras setup is visible in Figure 15.

Figure 15: Stereo camera setup installed on the portside rudder

3.3 Data post-processing

The obtained image quality exceeded all expectations: no motion blur was visible on the propeller blades at maximum speed and excellent cavitation images were delivered. An example captured during manoeuvring is visible in Figure 16.

During the operation of the propeller, non negligible rigid body motions of the whole propeller may occur due to deformation of the propeller and the rudder stock. A bronze reference area at the foot of the blade where rigid body motions but no deformations are present is set as a zero reference for the correction.

The main challenge encountered was the large amount of air bubbles generated by the bow of the ship especially when both propellers were engaged thus limiting the visibility and influencing the final test matrix. For this reason, the runs at higher speed with both propellers engaged did not produce reliable results and were discarded, despite the application of image averaging techniques. When only the composite propeller was engaged the image quality was excellent also at the highest speed. This is due to the induced drift angle that helped to clear the bubbles out of the cameras field of view.

In order to correlate two pictures, the same speckled area must be visible in both pictures: portions visible in only one camera are therefore excluded by the analysis. For this reason, air bubbles or cavitation on the propeller could reduce the usable area and generate noise in the measurements. In order to cope with this, an image averaging tool based on a median filter was developed using MATLAB® and applied. Averaging was also used during the tests in the cavitation tunnel; however, in that case surface averaging was used instead. The main

difference is that on the full scale data the averaging was applied on the raw image data instead to the processed blade surfaces obtained with DIC.

Figure 16: Cavitating tip and hub vortices at full scale during manoeuvring

An assessment was made of the effectiveness of the image averaging routine in filtering out the non-periodic propeller blade vibrations in comparison to the surface averaging method used during the tests in the cavitation tunnel. To do so, a routine able to automatically identify the images with the least disturbance from bubbles was used. The quality of the selected images was sufficient to carry out a separate DIC analysis for each image and the same surface averaging procedure described in 2.4.2 was applied. In parallel, the DIC analysis is carried out also for the pictures resulting from the image averaging of the raw image data obtained for each test.

The results obtained with surface averaging and image averaging are compared and the results indicate that the differences in the overall displacements between the two techniques are very small therefore proving the effectiveness of image averaging in handling non-periodic propeller vibrations. Furthermore, the measurement noise induced by bubbles, particles and cavitation is greatly reduced with this technique, strongly improving the quality of the data and enabling the usage of runs at higher speed.

3.3 Results

The measurement campaign successfully captured the deflection of the propeller blades at full scale. Measurement noise induced by small bubbles and particles is present in the raw data for all runs, but it is almost completely eliminated after the image averaging procedure. However, in cases where a large amount of bubbles obstruct the view, the image contrast on the blade surface is lowered at the outer radii, slightly increasing the measurement noise at these locations. Figure 17 shows an example of the obtained deflection patterns at increasing RPMs, while Figure 18 show the almost linear relation between tip displacements and torque. More details on the measurement results and their use in the validation of a BEM-FEM tool can be found in Maljaars et al (2019).

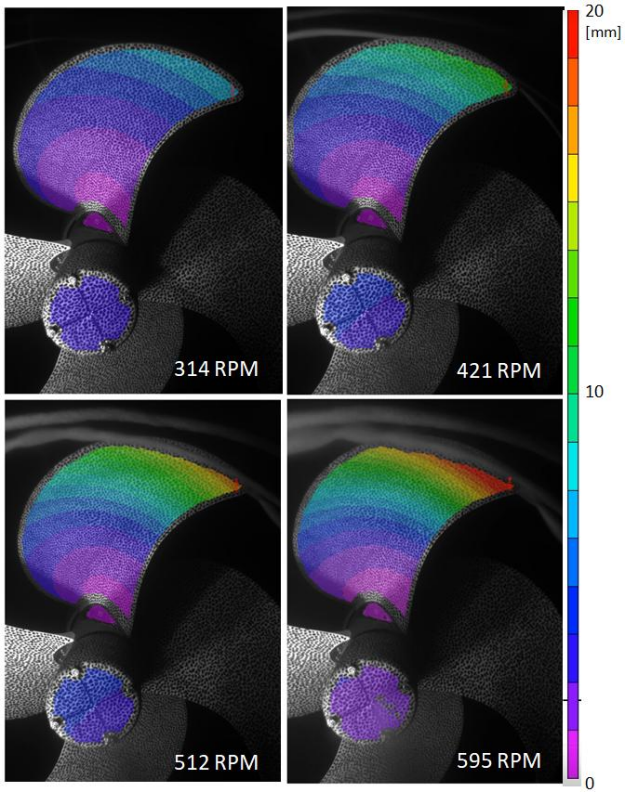

Figure 17: Propeller deflection with only one propeller engaged at increasing RPM. The measurement is carried out at the wake peak (12 o' clock).

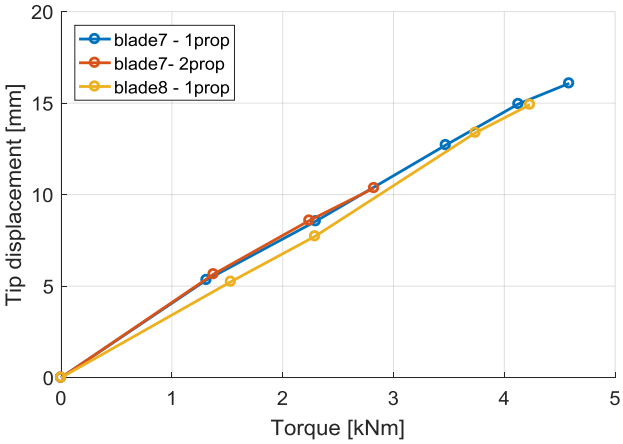

Figure 18: Tip displacement against torque for two propeller blades, with one (blue and yellow) or two propellers (red) engaged.

3.3.1 Assessment of measurement accuracy

The analysis of the expected measurement accuracy is carried out separately for the systemic accuracy related to the measurement system itself (e.g. resolution, camera's baseline distance, calibration errors etc) and the uncertainties induced locally by the presence of bubbles in the images.

The systemic measurement noise is assessed by analysing the measured deflections of different conditions with very

low RPM at the bronze portion of the blade root. Despite only a limited area is considered, this assessment at this location is conservative due to its low contrast and relatively poor illumination. The measurement accuracy is found equal to $D_{95\_systemic}$= ±0.03 mm assuming a Gaussian distribution of the measurement noise. This value decreases significantly if areas with better image contrast are chosen for the assessment and it is in line to what was expected based on the choices of camera positioning, optics and settings.

No effective way to quantitatively assess measurement bias was found due to the impossibility to apply fixed displacements to the propeller at full scale with a sufficient precision. However, as an educated guess based on the obtained results, DIC projection errors and the user's experience with DIC, such bias is expected to be negligible compared to the other sources of uncertainty.

The presence of air bubbles at the outer radii causes a reduction in the contrast after image averaging and therefore slightly lowering the measurement accuracy locally. Such decrease in measurement accuracy is assessed through a detailed analysis of the measured data: a cut along a line running from the blade root to the tip is generated in the displacement data and de-trended in order to isolate the measurement noise from the physical deformations. The resultant measurement noise show a clear increase in the outer radii, where most of the bubbles are present (see example in Figure 19). The recorded bubble-induced accuracy is found always below $D_{95\_bubbles}$= ±0.1 mm, and much lower values are recorded for the runs where less bubbles were present.

The sum of the base and bubble induced measurement noise leads to $D_{95\_overall}$= ±0.13 mm. Such value is typical for laboratory tests, therefore this is an extremely good result for full scale measurements.

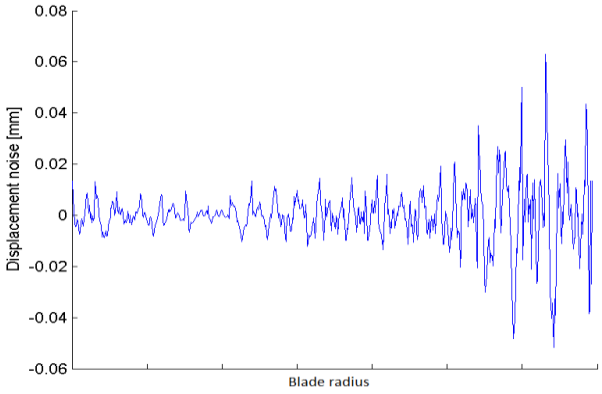

Figure 19: Measurement noise along the blade cut for one of the tests

4 CONCLUSIONS AND RECOMMENDATIONS

The following conclusions summarise the findings of the present work:

- A methodology to optically measure the hydro-elastic response of flexible propellers in non-uniform flow is developed and applied at model scale in the cavitation tunnel and at full scale on a ship.
- The measurements at model scale are achieved through an integrated approach including several techniques such as CFD optimization to design the wake field generator, Particle Image Velocimetry to assess the wake field and Digital Image Correlation to measure blade deformations.
- Good measurement data aimed at validation of BEM-FEM tools was gathered. Techniques such as surface and image averaging were used to filter out the non-periodic dynamics of the blades and reduce the disturbance of air bubbles and cavitation.
- Measurements for almost the full propeller rotation were achieved in the cavitation tunnel, enabling a good assessment of the influence of the wake field in the hydro-elastic response of the propeller blades.
- High measurement quality was achieved during both the measurement campaigns covered in this paper. The measurement noise achieved was D_{95}= ±0.06 mm and ±0.13 mm respectively for model and full scale. In particular, the measurement quality obtained at full scale exceeded all expectations.
- Propeller and cavitation observations were achieved at full scale with an unprecedented image quality.

ACKNOWLEDGMENTS

The authors would like to thank the participants of the Greenprop project (Delft University of Technology, Defence Material Organisation, Wärtsilä Netherlands B.V., Maritime Research Institute Netherlands, Solico B.V. and the Netherlands Organisation for Scientific Research) for their support. The authors gratefully thank the Royal Netherlands Navy for making the Nautilus available for the full scale measurement campaign.

REFERENCES

Adams, B. M., Ebeida, M. S., Eldred, M.S., Geraci,G., Jakeman, J.D., Maupin, K.A., Monschke J.A., Swiler, L.P., Stephens, J.A., Vigil, D.M., Wildey, T.M. (2017) "DAKOTA, A Multilevel Parallel Object-Oriented Framework for Design Optimization, Parameter Estimation, Uncertainty Quantification, and Sensitivity Analysis: Version 6.6 User's Manual"

Bosschers, J. (2017). 'A Semi-Empirical Method to Predict Broadband Pressure Fluctuations and Radiated Noise of Cavitating Tip Vortices'. Fifth International Symposium on Marine Propulsion, SMP 2017, Espoo, Finland.

Bunt van de, E., Lafeber, W. (2011). "Optical Measurement Techniques in Model Testing". Advanced Model Measurement Technology, AMT'11, Newcastle upon Tyne, United Kingdom.

Maljaars, P.J., Grasso, N., den Besten, H., Kaminski, M. (2019). 'BEM-FEM coupling for the analysis of flexible propellers in non-uniform flows and validation with full-scale measurements'. Journal of Fluids and Structures

Maljaars, P.J., Grasso, N., Kaminski, M., and Lafeber, W. (2017). "Validation of a steady BEM-FEM coupled simulation with experiments on flexible small scale propellers" Proceedings of the Fifth International Symposium on Marine Propulsion (SMP'17), Espoo, Finland.

Sterenborg, J., Grasso, N. and Tjallema, A. (2019). "The Ocean Cleanup System 001 performance during towing and seakeeping tests". Proceedings of the ASME 2019 38th International Conference on Ocean, Offshore and Arctic Engineering, OMAE2019, Glasgow, United Kingdom.

Sutton, J., Ortue, J. and Schreier, H. (2009). "Image Correlation for Shape, Motion and Deformation Measurements: Basic Concepts, Theory and Applications", Boston 1st Edition.

Vaz, G., Bosschers, J., Hoekstra, M., "Free-surface viscous flow computations. Validation of URANS code FRESCO" Proceedings of OMAE2009, Hawaii, USA, (2009).

Westerweel, J. 'Theoretical analysis of the measurement precision in particle image velocimetry'. Exp. Fluids 29 (2000) S3-12

Zondervan, G. J., Grasso, N., and Lafeber, W. (2017). "Hydrodynamic design and model testing techniques for composite ship propellers" Proceedings of the Fifth International Symposium on Marine Propulsion (SMP'17), Espoo, Finland.